Available online at www.sciencedirect.com

ScienceDirect

Geochimica et Cosmochimica Acta 71 (2007) 3833–3846

Geochimica et Cosmochimica Acta

www.elsevier.com/locate/gca

Equilibrium iron isotope fractionation factors of minerals: Reevaluation from the data of nuclear inelastic resonant X-ray scattering and Mössbauer spectroscopy

V.B. Polyakov [a,b,*], R.N. Clayton [c], J. Horita [b], S.D. Mineev [d]

[a] *Institute of Experimental Mineralogy, RAS, Chernogolovka, Moscow Region 142432, Russia*
[b] *Chemical Sciences Division, Oak Ridge National Laboratory, Oak Ridge, TN 37831-6110, USA*
[c] *Enrico Fermi Institute, Department of Chemistry and Department of the Geophysical Sciences, University of Chicago, Chicago, IL 60637, USA*
[d] *UralPlatinum Holding Ltd., Aviamotornaya 10/2, 111021 Moscow, Russia*

Received 31 July 2006; accepted in revised form 18 May 2007; available online 13 June 2007

Abstract

We have critically reevaluated equilibrium iron isotope fractionation factors for oxide and sulfide minerals using recently acquired data obtained by Mössbauer spectroscopy and inelastic nuclear resonant X-ray scattering (INRXS) synchrotron radiation. Good agreement was observed in the iron β-factors of metallic iron (α-Fe) and hematite calculated using both Mössbauer- and INRXS-derived data, which supports the validity and reliability of the calculations. Based on this excellent agreement, we suggest the use of the present data on the iron β-factors of hematite as a reference.

The previous Mössbauer-derived iron β-factor for magnetite has been modified significantly based on the Fe-sublattice density of states obtained from the INRXS experiments. This resolves the disagreement between naturally observed iron isotope fractionation factors for mineral pairs involving magnetite and those obtained from the calculated β-factors. The correctness of iron β-factor for pyrite has been corroborated by the good agreement with experimental data of sulfur isotope geothermometers of pyrite–galena and pyrite–sphalerite. A good correlation between the potential energy of the cation site, the oxidation state of iron and the iron β-factor value has been established. Specifically, ferric compounds, which have a higher potential energy of iron than ferrous compounds, have higher β-factors. A similar dependence of β-factors on the oxidation state and potential energy could be extended to other transition metals. Extremely low values of INRXS-derived iron β-factors for troilite and Fe_3S significantly widen the range of iron β-factors for covalently bonded compounds.

1. INTRODUCTION

The scope of studies of stable isotope geochemistry has been tremendously widened since the mid-1990s by the ever-growing development of multi-collector inductively coupled plasma mass-spectrometry (MC-ICP-MS). Isotopes of many chemical elements have become the subject of stable isotope geochemical investigations. A new field, non-traditional stable isotopes, has been established as a sub-discipline of isotope geochemistry (see Johnson et al., 2004a,b and references therein). Iron isotopes have attracted the most notice among the non-traditional stable isotopes, due to the high abundance of iron as well as its importance in a variety of geochemical and biogeochemical processes occurring over a wide range of temperatures and pressures, from the Earth's surface to the mantle and core.

Correct interpretation of natural and laboratory iron isotope data requires knowledge of equilibrium isotope fractionation factors as a *sine qua non* condition. Unlike many other non-traditional stable isotopes, the equilibrium fractionation factors of iron isotopes can be evaluated, within the framework of first-order thermodynamic perturbation

---

[*] Corresponding author.
E-mail address: polyakov@iem.ac.ru (V.B. Polyakov).

0016-7037/$ - see front matter © 2007 Elsevier Ltd. All rights reserved.
doi:10.1016/j.gca.2007.05.019

theory, from the experimental data of Mössbauer spectroscopy and/or inelastic nuclear resonant X-ray scattering (INRXS) in synchrotron radiation experiments. Data from Mössbauer spectroscopy were used for the first determination of the equilibrium isotope fractionation factors for iron (Polyakov, 1997). Regularities of the equilibrium iron isotope fractionation and its dependence on oxidation state were also first established from Mössbauer spectroscopy data (Polyakov and Mineev, 2000). Mass-spectrometric studies of natural samples, laboratory investigations and calculations confirmed these regularities for iron and other transition metal isotopes (Brantley et al., 2001; Matthews et al., 2001, 2004; Schauble et al., 2001; Walczyk and Von Blanckenburg, 2002; Rouxel et al., 2003, 2004, 2005; Anbar, 2004; Beard and Johnson, 2004a,b; Croal et al., 2004; Dauphas et al., 2004, 2007; Jarzęcki et al., 2004; Poitrasson et al., 2004, 2005; Schoenberg and Von Blanckenburg, 2004, 2006; Williams et al., 2004, 2005; Anbar et al., 2005; Balci et al., 2006; Dauphas and Rouxel, 2006; Dideriksen et al., 2006; Horn et al., 2006; Markl et al., 2006; Roskosz et al., 2006; Severmann et al., 2006; Busigny and Dauphas, 2007; Frost et al., 2007; Schuessler et al., 2007). However, some disagreements between Mössbauer-derived equilibrium fractionation factors and observed iron isotope fractionation factors from natural samples and in laboratory experiments were reported (Beard and Johnson, 2004a,b; Johnson et al., 2004a,b, 2005; Skulan et al., 2002; Wiesli et al., 2004; Yamaguchi et al., 2005).

Recently, Polyakov et al. (2005b) applied the INRXS synchrotron radiation technique to the determination of stable isotope fractionation factors of tin. This technique has some advantages over traditional Mössbauer spectroscopy and can provide more accuracy in the calculation of stable isotope fractionation factors. A combination of traditional Mössbauer spectroscopy and the INRXS synchrotron radiation technique allows one to obtain reliable values for stable isotope fractionation factors. In this paper, we provide a critical reevaluation of the iron stable isotope fractionation factors on the basis of the INRXS synchrotron radiation technique and Mössbauer spectroscopy. We have focused our attention on minerals that were studied recently in the literature, and compared INRXS- and Mössbauer-derived fractionation factors with iron isotope fractionation observed under experimental and natural conditions.

2. METHOD

2.1. First-order thermodynamic perturbation method

The reduced isotopic partition function ratio (β-factor), introduced by Bigeleisen and Mayer (1947) and Urey (1947), has been the main physical quantity in the theory of stable isotope fractionation. An equilibrium isotope fractionation factor between two substances A and B is expressed as:

$$\ln \alpha_{\mathrm{A-B}} = \ln \beta_{\mathrm{A}} - \ln \beta_{\mathrm{B}}, \tag{1}$$

where α is the equilibrium isotope fractionation factor and β is the β-factor. According to the definition, the β-factor can be written in terms of the Helmholtz free energy (Bigeleisen and Mayer, 1947; Urey, 1947; Singh and Wolfsberg, 1975):

$$z \ln \beta = -\frac{F^* - F}{RT} + \left(\frac{F^* - F}{RT}\right)_{\mathrm{class}}, \tag{2}$$

where F is the Helmholtz free energy (per mole); z is the multiplicity of isotope substitution (two for iron isotope substitution in the case of Fe_2O_3); T is absolute temperature; R is the universal gas constant. Hereafter, * relates to the isotopically substituted form and the subscript "class" marks quantities calculated in accord with classical mechanics.

Application of the first order thermodynamic perturbation theory to the stable isotope fractionation problem allows the β-factor to be expressed in the terms of the kinetic energy and the mass difference between the isotopes of interest (Polyakov, 1993, 1997; Polyakov and Kharlashina, 1994, 1995; Polyakov and Mineev, 2000; Polyakov et al., 2005a)

$$\ln \beta = \frac{\Delta m}{m^*}\left(\frac{\mathrm{KE}}{zRT} - \frac{3}{2}\right), \tag{3}$$

where KE is the kinetic energy (per one mole) of the sublattice of atoms of interest; m is the mass of isotope of interest; $\Delta m = m^* - m$.

Eq. (3) is derived from first principles and does not require any special assumptions and models. Eq. (3) is approximate, taking into account the first term that is linear with Δm, and neglecting terms which are proportional to quadratic and higher powers of Δm. Neglecting the higher terms is valid for all isotopes except for hydrogen and is based on the assumption of the ideal mixing of isotopes. This assumption is implicit in the great majority of the calculations of stable isotope fractionation factors of condensed matter (Polyakov, 1993). Eq. (3) provides a basis for calculating the β-factor of iron isotopes, using INRXS synchrotron radiation and Mössbauer data to calculate the kinetic energy of iron sublattices (Polyakov, 1997; Polyakov and Mineev, 2000; Polyakov et al., 2005a,b).

2.2. Mössbauer spectroscopy and inelastic nuclear resonant X-ray scattering

Mössbauer spectroscopy provides experimental data that can be used to calculate the β-factor. Historically, the first determination of equilibrium iron isotope fractionation factors was made using data obtained from Mössbauer spectroscopy (Polyakov, 1997). The second-order Doppler (SOD) shift in Mössbauer spectra is proportional to the vibrational kinetic energy of the Mössbauer-sensitive isotope (e.g. ^{57}Fe):

$$S = -\mathrm{KE}/mc, \tag{4}$$

where S is the SOD shift (in velocity units); c is the speed of light.

Substituting Eq. (4) in Eq. (3) results in a simple equation expressing the β-factor in terms of the experimentally measurable quantity, namely, the SOD shift in Mössbauer spectra (Polyakov, 1997):

$$\ln\beta = \frac{\Delta m}{m^{*}}\left(-\frac{mSc}{zRT} - \frac{3}{2}\right). \tag{5}$$

The mass m in (5) should be expressed in amu, $m = 57$, in the case of iron.

The SOD shift is responsible for temperature shifts observed in Mössbauer spectra. Therefore, experimental determination of the SOD shift (and, consequently, calculation of the β-factor) requires Mössbauer spectroscopic measurements at different temperatures. To extract the SOD shift from the Mössbauer spectra at different temperatures some assumptions on the temperature dependence of SOD shift are needed. This introduces some errors in the Mössbauer-derived SOD shift. Another source of error in the Mössbauer-derived SOD shift is the temperature dependence of the isomeric shift, which can be confused with the SOD shift. Fortunately, the temperature dependence of the isomeric shift is usually (but not always) small in comparison with the SOD shift and does not distort significantly the true value of the SOD shift.

Polyakov et al. (2005b) presented and applied a new method for experimentally determining the kinetic energy (KE) of elements having Mössbauer-sensitive isotopes (tin isotopes as an example). One can apply this method directly to iron isotopes. The experimental foundation is based on recent progress in nuclear resonant scattering of synchrotron X-radiation, which, together with the development of high-resolution X-ray monochromators, allows one to measure energy spectra of nuclear resonant inelastic absorption directly (e.g. Chumakov and Sturhahn, 1999). This technique provides the possibility of obtaining the phonon partial density of states (PDOS) for the resonant atom (Sturhahn et al., 1995, 1998; Kohn and Chumakov, 2000; Alp et al., 2001).[1] The PDOS is extracted from the observations of Mössbauer resonant photons scattered by thermal phonons in single-phonon processes. The high-resolution monochromator provides a 0.8 meV resolution in the energy of the scattered photons and allows one to obtain ~100 columns in the PDOS histogram, which is usually 80–100 meV wide. ($1\ \text{meV} = 10^{-3}\ \text{eV} = 1.60217653 \times 10^{-22}\ \text{J} \approx 8.06602\ \text{cm}^{-1} \approx 2.41814 \times 10^{11}$ Hz). The extraction procedure of the PDOS from the energy spectra of nuclear resonant inelastic absorption includes the double Fourier transform, which allows one to eliminate the multiphonon contribution together with the deconvolution of the data (Kohn et al., 1998). The general approach is based on two main approximations: (a) the adiabatic approximation in which the motion of heavier ion cores is treated separately from that of the electrons, whose average motion generates the potential that dictates the motion of the ion cores; and (b) the harmonic approximation in which only the second-order term in the Taylor expansion of the interatomic potential is retained (Alp et al., 2001). It should be emphasized that the PDOS represents the vibrational energy spectrum of the Mössbauer-sensitive isotope (^{57}Fe in the case of iron) for which the resonant nuclear scattering is observed. Since the PDOS of the iron sublattice is known, all atomic thermal properties of the sublattice such as vibrational energy and heat capacity as well as Mössbauer quantities such as the Lamb–Mössbauer (LM) factor or SOD shift can be computed using standard statistical physics formulas. Thermodynamic properties of the iron sublattice from PDOS are computed in a completely analogous way to the computation of the thermodynamic properties of the total crystal from a complete DOS. According to Eq. (3), the kinetic energy of the iron sublattice is the main physical quantity needed for the computation of iron isotope β-factors.

If the PDOS of an atom of interest is known from INRXS experiments, the kinetic energy can be calculated from the following equation:

$$\mathrm{KE} = 3/2 \int_0^{e_{\max}} E(e/kT)g(e)\,\mathrm{d}e \tag{6}$$

where $g(e)$ is the PDOS, $E(e/kT)$ is the Einstein function for the vibrational energy of a harmonic oscillator having the frequency $v = e/h$, h is the Planck constant, $e_{\max}$ is the maximal energy of the vibration spectrum (blue limit). The Einstein function is given by

$$\frac{E(e/kT)}{kT} \equiv \frac{e/kT}{\exp(e/kT) - 1} + 0.5e/kT \tag{7}$$

Eqs. (6) and (7) are valid under the harmonic approximation and Eq. (6) takes into account the virial harmonic relation $K = 0.5E_{\text{vib}}$, where E_{vib} is the vibrational energy of the harmonic oscillator. The PDOS function is normalized to unity:

$$\int_0^{e_{\max}} g(e)\,\mathrm{d}e = 1 \tag{8}$$

Eqs. (3), (6)–(8) allow computing the β-factor if the PDOS is found from the INRXS in synchrotron radiation experiments. The INRXS radiation technique provides more reliable β-factors than those derived by Mössbauer spectroscopy. In distinction from Mössbauer SOD shift measurements, the INRXS radiation experiments are conducted at a single temperature, which avoids the possibility of confusing the SOD shift with the temperature dependence of the isomeric shift. The INRXS-based computation also does not require any model assumptions about the type of vibrational spectrum and/or interatomic potential. Mössbauer spectroscopy and INRXS approaches for the determination of the iron isotope β-factors are based on different model assumptions. Thus, an agreement between Mössbauer- and INRXS-derived iron isotope β-factors provides compelling evidence for the validity of the calculations.

---

[1] The vibrational spectrum or density of state (DOS) is the most valuable physical quantity for the calculations of thermodynamic properties of solids. If the DOS is known, any thermodynamic property can be computed using appropriate equations of statistical physics (e.g. Maradudin et al., 1971). The PDOS is the part of the DOS relating to vibrations of the sublattice of an element of interest. The PDOS presents the energy spectrum of the sublattice thermal vibrations. Using the PDOS, the thermodynamic properties of the sublattice such as the kinetic energy, the contribution to heat capacity, etc. can be computed.

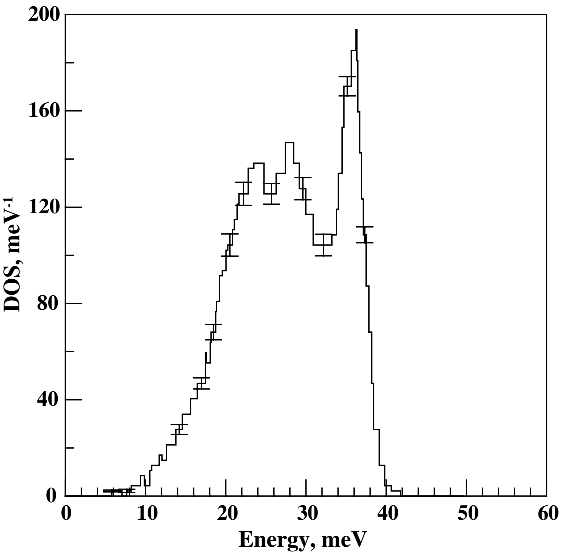

Fig. 1. The phonon DOS of metallic iron (α-Fe) (Alp et al., 2001). Typical uncertainties in the phonon DOS values are shown by error bars.

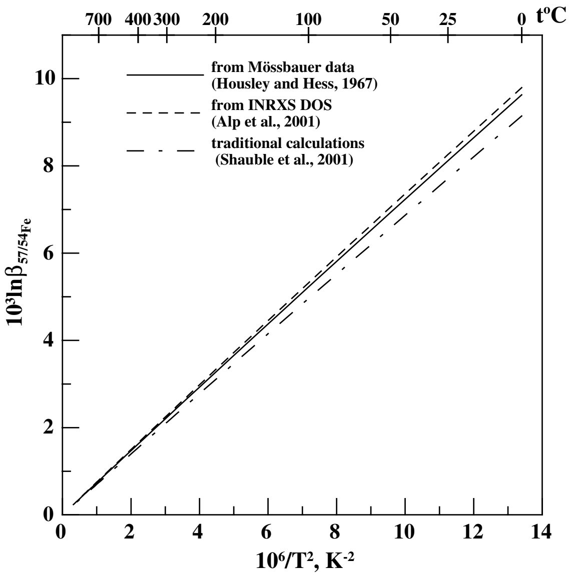

Fig. 2. Comparison of Mössbauer- and INRXS-derived β-factors of metallic iron (α-Fe). Error bars show typical uncertainties in the β-factors of metallic iron resulted from the uncertainties in the phonon DOS of metallic iron. The method for calculations of the iron β-factor uncertainties is presented by Polyakov et al. (2005b).

3. RESULTS

In this section, we present our new calculations of the iron isotope β-factors for iron-bearing compounds using INRXS data on PDOS and new Mössbauer spectroscopy data. These new computations complement and revise early calculations by Polyakov (1997) and Polyakov and Mineev (2000).

3.1. Metallic iron (α-Fe)

Metallic iron is the most thoroughly studied substance by both Mössbauer spectroscopy and the INRXS synchrotron radiation technique. Mössbauer spectroscopic studies of metallic iron were carried out intensively in the early stages of investigations of the Mössbauer effect. Housley and Hess (1967) summarized these investigations and obtained an accurate SOD shift for metallic iron. Their results can be well approximated by a Debye function with the characteristic temperature $\theta_M = 421 \pm 10$ K. There are several INRXS synchrotron radiation studies of metallic iron (Sturhahn et al., 1995; Chumakov et al., 1996; Toellner et al., 1997; Chumakov and Sturhahn, 1999; Kohn and Chumakov, 2000; Alp et al., 2001; Shen et al., 2004). The phonon DOS[2] histogram for metallic iron is shown in Fig. 1. Unlike traditional Mössbauer spectroscopy, the INRXS technique does not require measurements at different temperatures. We have used both types of data to compute the temperature dependence of the β-factor of metallic iron, using Eq. (5) in the case of the SOD shift measurements and Eqs. (3), (6)–(8) in the cases when the phonon DOS is available. Results of the computations are presented in Fig. 2, together with conventional calculations by Schauble et al. (2001) for comparison. Uncertainties in the INRXS-derived β-factors were calculated by the method described by Polyakov et al. (2005b). One can see good agreement between Mössbauer- and INRXS-derived β-factors for metallic iron. Small differences are within the range of experimental and computational error. The three-term polynomial expressions for 57/54 and 56/54 β-factors for α-iron in Table 1 are computed according to Housley and Hess (1967). The polynomial expression is valid at temperatures above 273 K (0 °C) and agrees with the corresponding polynomial of Polyakov and Mineev (2000).

3.2. Iron oxides

3.2.1. Hematite (α-Fe_2O_3)

The SOD shift of hematite was obtained by both traditional Mössbauer spectroscopy and synchrotron radiation experiments. The temperature dependence of the SOD shift of synthetic hematite is described by a Debye function with $\theta_M = 500 \pm 40$ K (De Grave and Van Alboom, 1991). This value for θ_M was confirmed by Polyakov et al. (2001), who found $\theta_M = 502 \pm 25$ K. The SOD shift was also estimated from the INRXS experiments directly using a special technique (Chumakov and Sturhahn, 1999; Kohn and Chumakov, 2000). As in the case of PDOS determination, one can obtain the SOD shift from an INRXS synchrotron experiment at one temperature instead of wide range of temperatures in the case of Mössbauer spectroscopy. A comparison between β-factors computed from the SOD shifts mentioned above is shown in Fig. 3. An excellent agreement between traditional Mössbauer- and INRXS-derived iron isotope β-factors for hematite strongly supports the use of hematite iron isotope β-factors as reference data for com-

---

[2] The PDOS coincides with the DOS in the case of single-element substances.

Table 1
Polynomial coefficients for calculating iron β-factors of minerals under study

Solids	Method and source	Coefficients of the polynomial expansion: $10^3 \ln \beta = \sum_{i=1}^{3} A_i x^i,\ x_i = 10^6/T^2$					
		$^{57}Fe/^{54}Fe$			$^{56}Fe/^{54}Fe$		
		A_1	$A_2 \times 10^3$	$A_3 \times 10^6$	A_1	$A_2 \times 10^3$	$A_3 \times 10^6$
Iron metal	Mössbauer-derived from Housley and Hess (1967)	0.69964	−1.4762	4.8454	0.47475	−1.0017	3.2879
Hematite	Mössbauer-derived from Polyakov et al. (2001)	1.0542	−3.1652	1.3260	0.71534	−2.1478	8.9976
Magnetite	INRXS-derived from Seto et al. (2003)	0.95706	−4.7296	4.0703	0.64943	−3.2094	2.7620
FeO (wüstite)	INRXS-derived from Struzhkin et al. (2001, 2004)	0.67154	−2.2631	1.4589	0.45569	−1.5357	9.8995
Pyrite	Mössbauer-derived from Nishihara and Ogawa (1979)	1.5729	−7.0581	4.2873	1.0673	−4.7894	2.9093
Marcasite	Mössbauer-derived from Permyakov et al. (2004)	1.3430	−5.4604	3.3409	0.91129	−3.7053	2.2670
Troilite	INRXS-derived from Kobayashi et al. (2004)	0.43820	−9.8632	4.4614	0.29735	−6.6929	3.0274
Fe_3S	INRXS-derived from Lin et al. (2004)	0.47319	−8.5917	2.6653	0.32109	−5.8301	1.8086

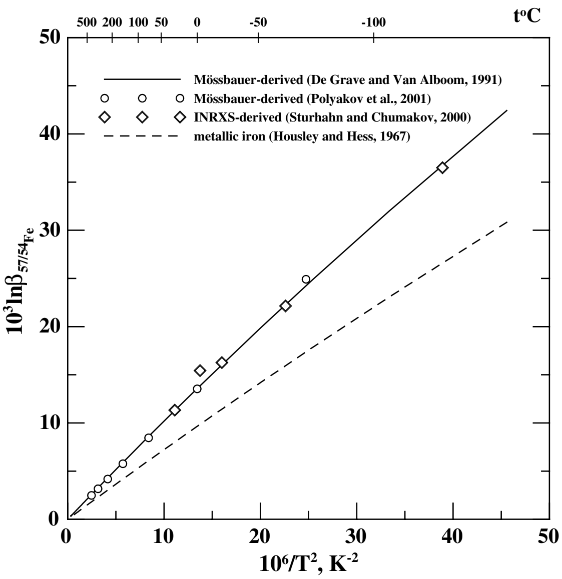

Fig. 3. Mössbauer- and INRXS-derived iron β-factors for hematite (α-Fe_2O_3). Metallic iron is presented for comparison.

parisons of calculated, experimental or natural iron isotope fractionation factors. The three-term polynomial, based on Polyakov et al. (2001), is presented in Table 1, which agrees with the previous expressions of Polyakov and Mineev (2000).

3.2.2. *Magnetite (Fe_3O_4)*

Polyakov and Mineev (2000) computed magnetite β-factors from Mössbauer SOD data of De Grave et al. (1993) and Persoons et al. (1993). De Grave et al. (1993) and Persoons et al. (1993) reported extremely high values of $\theta_M = 665 \pm 25$ K for the A site (Fe^{3+}) and $\theta_M = 570 \pm 15$ K for the B site ($Fe^{2+} + Fe^{3+}$).

Recently, Seto et al. (2003) presented the INRXS-derived PDOS for magnetite (Fig. 4). We calculated the temperature dependence of the magnetite β-factor from the PDOS reported by these authors. A comparison of the magnetite β-factors calculated from data cited above is given in Fig. 5. There is clearly a large difference between β-factors computed from the Persoons et al. (1993) measurements and those obtained from other sources. It appears that the Mössbauer data of magnetite by Persoons et al. (1993) are suspect. The three-term polynomial, presented in Table 1, corresponds to magnetite β-factors computed from the Seto et al. (2003) INRXS-derived PDOS. This new equation differs significantly from the previous one calculated by Polyakov and Mineev (2000), using Mössbauer data of Persoons et al. (1993).

3.2.3. *FeO (wüstite)*

Struzhkin et al. (2001, 2004) obtained the iron PDOS of FeO (wüstite) from synchrotron radiation experiments for INRXS at pressures from 0.9 to 49 GPa. They observed substantial softening of the PDOS at energies below 10 meV at pressures 15–20 GPa, which persisted at high pressures up to 49 GPa. They related the observed softening to the magnetoelastic coupling in the high-pressure antiferromagnetic phase. In principle, the PDOS data at different pressures allows one to estimate the pressure dependence of

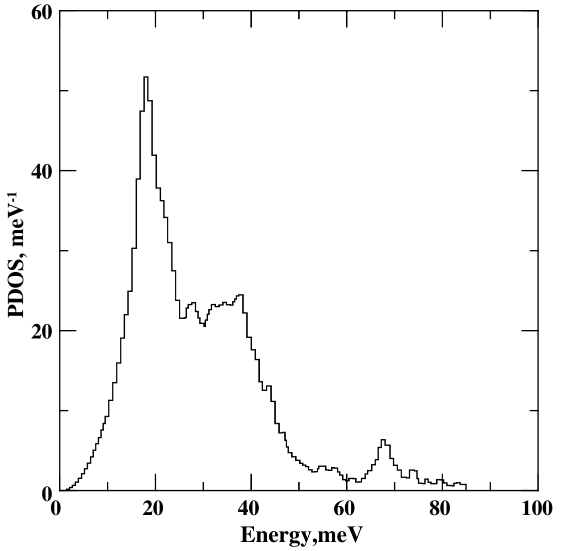

Fig. 4. The PDOS of Fe in magnetite, obtained by Seto et al. (2003) in INRXS synchrotron radiation experiments. The PDOS, presented here, is the resultant density of vibration energy for iron nuclei in A- and B-sites.

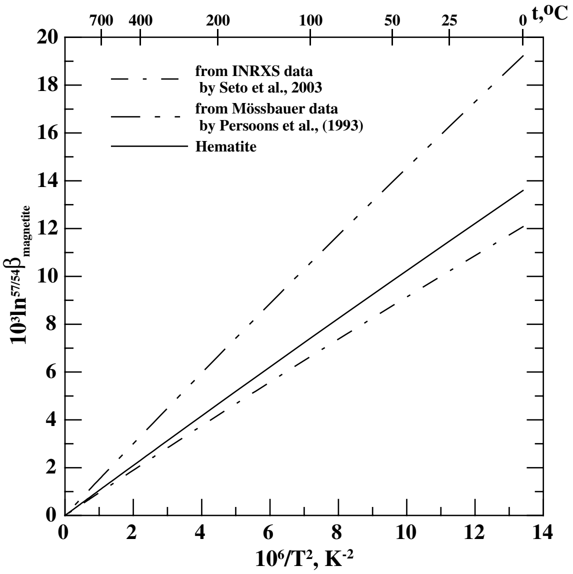

Fig. 5. Comparison of Mössbauer- and INRXS-derived iron β-factors for magnetite. One can see significant differences between magnetite β-factors computed from Persoons et al. (1993) Mössbauer spectroscopy data and those computed from INRXS data of Seto et al. (2003) and Permyakov et al. (2004). β-Factors for hematite are presented for comparison.

iron β-factors for FeO. However, a detailed study of the pressure dependence of iron β-factors for FeO lies beyond the scope of the present paper. We have computed the iron β-factors for FeO using the iron PDOS (Fig. 6) measured by Struzhkin et al. (2001, 2004) at 0.9 GPa, the lowest pressure in their studies, at which the pressure effect for the iron FeO β-factors does not exceed 0.15‰ at room temperature. The temperature dependence of the iron β-factor for FeO is shown in Fig. 7 and an appropriate polynomial expression is presented in Table 1.

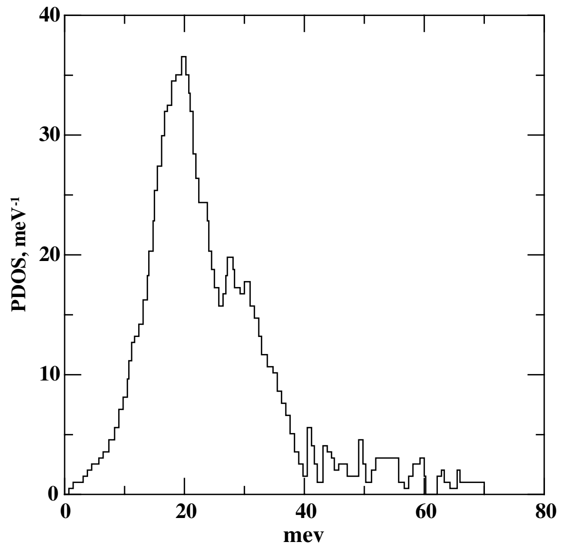

Fig. 6. The PDOS of FeO (wüstite) at 0.9 GPa after Struzhkin et al. (2001, 2004).

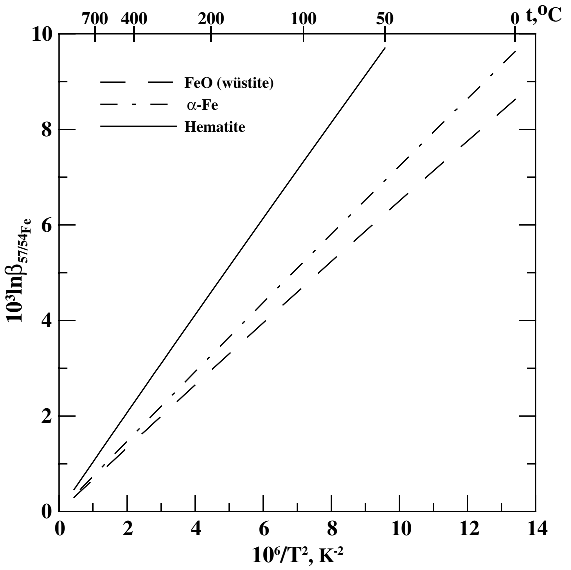

Fig. 7. Temperature dependence of the iron β-factor for FeO (wüstite) from PDOS obtained by Struzhkin et al. (2001, 2004). β-factor values relate to pressure 0.9 GPa. Temperature dependence of iron β-factors for α-Fe and hematite are presented for comparisons.

3.3. Iron sulfides

Iron β-factors for pyrite were previously estimated by Polyakov and Mineev (2000), using the SOD data of Mössbauer measurements for a synthetic sample of pyrite by Nishihara and Ogawa (1979). New iron β-factors for pyrite were recently published by Permyakov et al. (2004) based on the Mössbauer investigations of natural pyrite samples. These data along with new INRXS-derived iron β-factors for troilite and other iron sulfides expand the range of possible variations of the iron isotope composition in equilibrium isotope fractionation processes involving sulfides.

3.3.1. Pyrite (FeS_2)

Permyakov et al. (2004) presented results of Mössbauer investigations of natural pyrite from the Butuobin deposit in Russia. Iron is distributed among pyrite (~76%), marcasite (~14%) and an unidentified phase (presumably arsenopyrite, 10%) according to Mössbauer spectra and X-ray phase analysis. The SOD was described in terms of the Debye model. The following values for characteristic temperatures, θ_M, were obtained: 598 ± 12 K for pyrite and 516 ± 26 K for marcasite. The temperature dependence of the iron β-factor for pyrite and marcasite are presented in Fig. 8 in comparison with the pyrite β-factor from Nishihara and Ogawa (1979). From Fig. 8, one can observe good agreement between the data of Nishihara and Ogawa (1979) for the β-factor for pyrite ($\theta_M = 610 \pm 20$) and those obtained by Permyakov et al. (2004).

3.3.2. Troilite and Fe_3S

The INRXS spectrum for troilite published recently by Kobayashi et al. (2004) is presented in Fig. 9. The iron

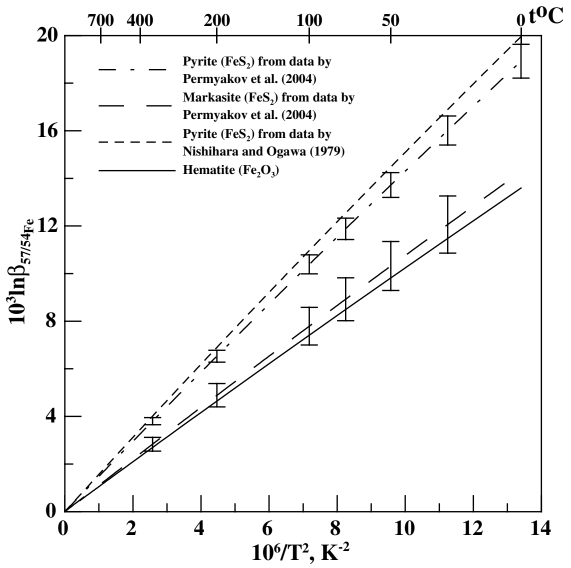

Fig. 8. Mössbauer-derived β-factors from the natural sample of pyrite (Permyakov et al., 2004). Along with pyrite, the sample contains marcasite (~14 mass%) and about 10 mass% of an unidentified phase, possibly arsenopyrite according to Mössbauer spectroscopic data. Error bars for pyrite and marcasite reflect uncertainties in Mössbauer temperatures: 598 ± 12 K for pyrite and 516 ± 26 K for marcasite.

sublattice PDOS relates to a pressure of 1.5 GPa. The temperature dependence of the iron β-factor for troilite is shown in Fig. 10 and the third-order polynomial is presented in Table 1. The PDOS of troilite was measured at different pressure and the pressure effect on the iron β-factor for troilite can be estimated, in principle. However, this subject lies beyond the scope of the present paper. The iron β-factor for troilite is much lower than those for pyrite and marcasite presented in Fig. 10 for comparison.

Fe_3S is the most iron-rich sulfide mineral currently known. It forms at 21 GPa and 1300 K. This compound may play an important role in the formation of cores in the Earth and Mars (Poirier, 1994; Bertka and Fei, 1998). Lin et al. (2004) measured INRXS spectra of Fe_3S at pressures up to 57 GPa. The PDOS at ambient pressure is presented in Fig. 11. The temperature dependence of the iron isotope β-factor (Fig. 10) is close to, but somewhat larger than, that for troilite (FeS).

4. DISCUSSION

4.1. Correlation with the electrostatic energy

The INRXS using synchrotron radiation and Mössbauer spectroscopy are complementary methods for the determination of iron isotope β-factors. The INRXS method provides more accuracy, but Mössbauer spectroscopy is a site-specific technique, which allows the determination of internal equilibrium isotope fractionation in a mineral.

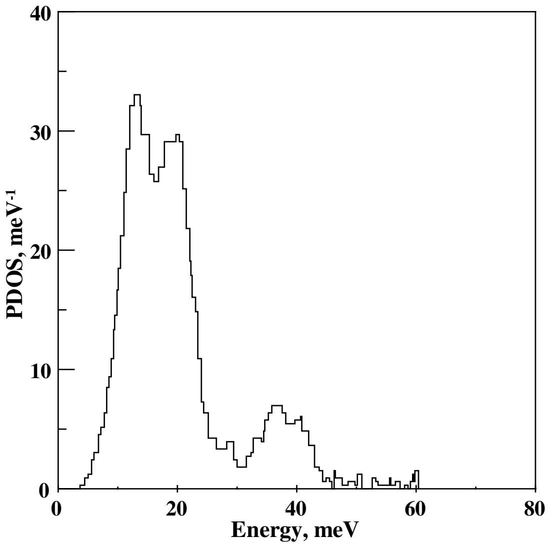

Fig. 9. The PDOS of troilite from INRXS synchrotron radiation experiments (Kobayashi et al., 2004).

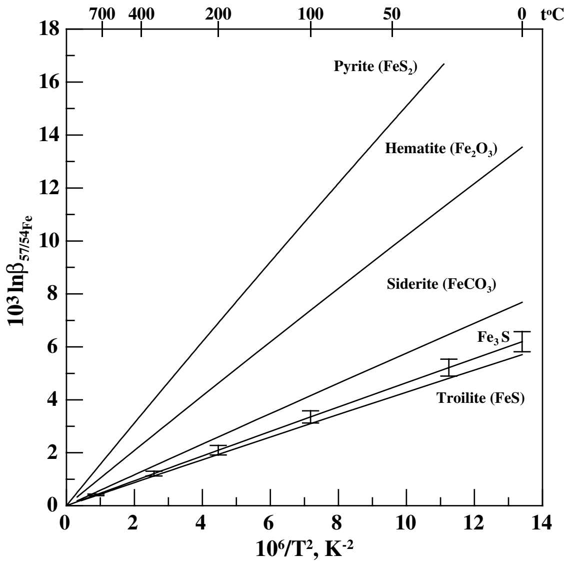

Fig. 10. The temperature dependence of the iron β-factors for troilite (FeS) and Fe_3S. The iron β-factors for pyrite, hematite and siderite are presented for comparison. The range of equilibrium iron isotope fractionation for sulfides is extremely wide and even exceeds typical difference between the iron β-factors of ferric and ferrous compounds. The iron β-factors for siderite were calculated using $\theta_M = 375$ K as suggested by De Grave and Van Alboom (1991). Uncertainties in the iron β-factors for Fe_3S, which are typical for IRNXS-derived values, results from uncertainties in the PDOS (Fig. 11). The method for calculations of the iron β-factor uncertainties is presented by Polyakov et al. (2005b).

The use of Mössbauer-derived and INRXS-derived results provides a powerful tool for obtaining reliable data on iron isotope β-factors of minerals. Agreement of β-factor values obtained by the two different techniques (e.g., metallic iron and hematite) provides confidence in the accuracy of these values. We believe that an excellent agreement

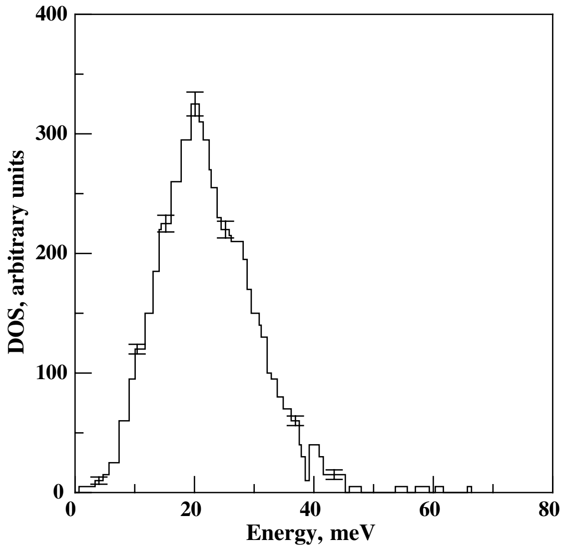

Fig. 11. The iron-sublattice PDOS of Fe_3S (Lin et al., 2004). Typical uncertainties in the PDOS values are shown by error bars.

between INRXS- and Mössbauer-derived iron β-factors obtained from different studies (Fig. 3) allows us to use hematite as a reference mineral for equilibrium iron isotope fractionation. The present study reveals the serious disagreement between the previous Mössbauer-derived iron isotope β-factors for magnetite (Polyakov and Mineev, 2000) and our new calculations in this study based on the PDOS results from INRXS with synchrotron radiation technique (Fig. 5); the Mössbauer-derived β-factors are much greater than the corresponding INRXS-derived values.

Our INRXS-based re-evaluation of the iron isotope fractionation factors confirms the main regularity in equilibrium iron isotope fractionation factors, namely dependence on the oxidation states, as was previously observed from the Mössbauer spectroscopic data (Polyakov and Mineev, 2000). The INRXS-derived iron β-factors for FeO (wüstite), which is a typical value for Fe^{2+} compounds, are smaller than those for hematite and metallic iron. The dependence of the iron isotope β-factors on oxidation state is shown as a correlation between the iron β-factor and the electrostatic site energy calculated by the method of Smyth (1989) (Fig. 12). Such a correlation was also observed for oxygen isotope fractionation factors in silicates (Smyth and Clayton, 1988; Clayton et al., 1989; Rosenbaum et al., 1994; Chacko et al., 1996). As one can see in Fig. 12, the potential energy of the ferric sites is about twice that of ferrous sites. It is known that stronger bonded compounds are characterized by larger values of the β-factor (e.g. Singh and Wolfsberg, 1975). Therefore, the ferric compounds (or sites) have β-factors that are larger than those for ferrous ones. It is interesting to compare values for the iron β-factor of magnetite from Polyakov and Mineev (2000) and those in this paper. One can see that the present calculations obey the trend shown in the figure, while the calculations of Polyakov and Mineev (2000) using the Mössbauer data of De Grave et al. (1993) and Persoons et al. (1993) do not.

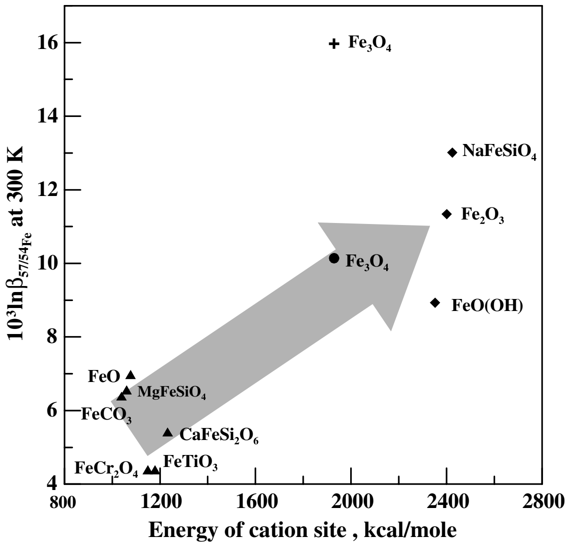

Fig. 12. Correlation between electrostatic energy of iron site and iron β-factor. Diamonds and triangles refer to ferric and ferrous compounds, respectively; magnetite data are marked as a cross (Mössbauer-derived from De Grave et al. (1993) and Persoons et al. (1993)) and a square (INRXS-derived from Seto et al. (2003)). The energies of cation site were taken from Smyth and Bish (1988). The energies and the β-factors for magnetite were computed by averaging data on A and B magnetite sites with weight coefficients 1 and 2, respectively. The iron β-factors for minerals except hematite, FeO (wüstite) and INRXS-derived magnetite are taken from Polyakov and Mineev (2000). Hematite, FeO (wüstite) and INRXS-derived magnetite β-factors obtained in this study. One can see that β-factor value for magnetite calculated by Polyakov and Mineev (2000) from the characteristic temperatures θ_M obtained by De Grave et al. (1993) and Persoons et al. (1993) does not obey the trend describing correlation between the electrostatic energy of the iron sites and iron β-factors.

4.2. Comparison with experimental and natural data

It has been previously observed (e.g. Johnson et al., 2003) that iron isotope fractionation factors between minerals calculated based on the Mössbauer spectroscopy (Polyakov and Mineev, 2000) appear to be overestimated compared to those based on experimental and natural studies. This apparent discrepancy is due mainly to an overestimation of the iron β-factor for magnetite computed by Polyakov and Mineev (2000), because of their use of the SOD shift presented by De Grave et al. (1993) and Persoons et al. (1993). In Table 3, we compared the "preferred" isotope fractionation factors presented by Johnson et al. (2003) with our new calculations for magnetite and other minerals in this study, obtained from new sets of Mössbauer-spectroscopy and INRXS data (Table 2). We present iron isotope fractionation factors between minerals, rather than those with respect to dissolved iron (Johnson et al., 2003). One can observe overall agreement between "preferred" values of Johnson et al. (2003) and calculated equilibrium iron isotope fractionation factors in this study (Table 2). We emphasize that large non-systematic variations in iron isotope compositions of minerals from banded iron formations from the Transvaal Craton studied by Johnson et al. (2003) reflect iron isotope fractionation in multistage forming processes and suggest that many mineral phases are not in equilibrium.

Frost et al. (2007) tested the agreement between INRXS- and Mössbauer-derived β-factors and iron isotope mineral–mineral fractionation including magnetite using natural samples from the Biwabik Iron Formation. They pointed out the agreement for magnetite–silicate (hedenbergite) and magnetite–carbonate (siderite) at high temperatures (>550 °C), but did not observe any temperature regularities in iron isotope fractionation coefficients between minerals at low temperatures. They suggested that equilibrium state was not attained at low temperatures. The iron isotope fractionation between magnetite and pyroxene at 750 °C observed by Dauphas et al. (2004) for natural samples from Early Archean band iron formation from Greenland are also in agreement with β-factors for magnetite computed in this study and those for pyroxene from Polyakov and Mineev (2000).

It is also interesting to compare INRXS- and Mössbauer-derived β-factors with laboratory iron isotope investigations. We devote our attention to mineral–mineral equilibrium isotope fractionation factors only, so as to avoid using available theoretical calculations of β-factors for aqueous iron complexes, which contradict each other. (e.g. Anbar et al., 2005; Schauble et al., 2001). Available experimental data allow us to determine of magnetite–hematite and magnetite-siderite $^{56/54}$Fe isotope fractionations at room temperatures. To find the magnetite–hematite $^{56/54}$Fe isotope fractionation factors ($\Delta^{56/54}\mathrm{Fe}_{\text{hem-mag}}$), the following experiments can be used:

- the $^{56/54}$Fe fractionation factor between ferric aqua complexes and hematite at 98 °C, $\Delta^{56/54}\mathrm{Fe}_{\text{Fe(III)aq-hem}} = -0.1‰$ (Skulan et al., 2002);
- the $^{56/54}$Fe fractionation factor between ferric and ferrous aqua complexes at 22 °C, $\Delta^{56/54}\mathrm{Fe}_{\text{Fe(III)aq–Fe(II)aq}} = +3.0‰$ (Welch et al., 2003);
- the $^{56/54}$Fe fractionation factor between ferrous aqua complexes and magnetite at 22 °C, $\Delta^{56/54}\mathrm{Fe}_{\text{Fe(II)aq-mag}} = -1.3‰$ (Johnson et al., 2005).

One can see that $\Delta^{56/54}\mathrm{Fe}_{\text{Fe(III)aq-hem}}$ was measured at 98 °C, whereas all other fractionation factors relate to 22 °C. To reduce all experiments to the same temperature, we used the temperature dependence of the hematite and ferric aqua complex β-factors:

$$\begin{aligned}\Delta^{56/54}\mathrm{Fe}_{\text{Fe(III)aq-Hem}}(22\,^\circ\mathrm{C}) &= \Delta^{56/54}\mathrm{Fe}_{\text{Fe(III)aq-Hem}}(98\,^\circ\mathrm{C}) \\ &+10^3\Big[(\ln^{56/54}\beta_{\text{Fe(III)aq}}(22\,^\circ\mathrm{C}) - \ln^{56/54}\beta_{\text{Fe(III)aq}}(98\,^\circ\mathrm{C})) \\ &-(\ln^{56/54}\beta_{\text{Hem}}(22\,^\circ\mathrm{C}) - \ln^{56/54}\beta_{\text{Hem}}(98\,^\circ\mathrm{C}))\Big] \qquad (9)\end{aligned}$$

$10^3(\ln^{56/54}\beta_{\text{Fe(III)aq}}(22\,^\circ\mathrm{C}) - \ln^{56/54}\beta_{\text{Fe(III)aq}}(98\,^\circ\mathrm{C})) = 3.37$ according to DFT-based calculations by Anbar et al. (2005). It is likely that temperature dependence of the calculated β-factor for ferric aqua complexes in the relatively narrow temperature range from 98 to 22 °C is more accurate than calculations of the absolute β-factor values.

Table 2
Comparison between Mössbauer- and INRXS-derived equilibrium iron (56/54) isotope fractionation factors and isotope fractionation factor from Johnson et al. (2003) for minerals

	T (°C)	ln $\alpha_{\text{A–B}}$, ‰[a]					
		Siderite		Magnetite		Hematite	
		Equilibrium	Johnson et al. (2003)	Equilibrium	Johnson et al. (2003)	Equilibrium	Johnson et al. (2003)
Ankerite	25	−1.5 (−0.3)	0 to −3.5 median: −1.75	−3.7 (−2.5)	−2.1 to −4.3 median: −3.2	−4.5 (−3.1)	−3.1 to −4.6 median: −3.85
	100	−1.0 (−0.2)	0 to −2.0 median: −1.0	−2.5 (−1.5)	−2.1 to −4.3 median: −3.2	−3.0 (−2.0)	−1.8 to −3.0 median −2.4
Siderite	25			−2.4 ± 0.4	−0.7 to −2.8 median: −1.7	−3.0 ± 0.4	−0.9 to −2.9 median: −1.9
	100			−1.5 ± 0.25	−0.4 to −1.8 median: −1.1	−2.0 ± 0.3	−0.7 to −2.0 median: −1.35
Magnetite	25					−0.8 ± 0.4	−0.3 to −0.4 median: −0.35
	100					−0.5 ± 0.25	−0.1 to −0.2 median: −0.15

Isotope fractionation factors between minerals A and B can be found in the cell at the intersection of the row relating to the mineral A and the column relating to the mineral B. All "Johnson et al., 2003" isotope fractionation factors are computed from the "preferred" values presented in Table 3 of that paper by excluding values for dissolved Fe^{2+} and Fe^{3+}. For example, to find the "Johnson et al., 2003" value for the ankerite–siderite pair, one must subtract the Fe^{2+}–ankerite "preferred" value from the Fe^{2+}–siderite "preferred" value. This is also true for the equilibrium values except fractionation factors for pairs involving magnetite. We have used new values for the magnetite β-factor calculated in this study instead of the incorrect β-factor for magnetite from Polyakov and Mineev (2000) used by Johnson et al. (2003). Since the iron β-factors are known for two ankerites having different elemental composition: $CaFe_{0.5}Mg_{0.5}(CO_3)_2$ and $Ca_{1.1}Mg_{0.5}Fe_{0.3}Mn_{0.1}(CO_3)_2$, equilibrium fractionation factors for the second composition of ankerite are presented in parentheses.

[a] A is a mineral in the first column; B is a mineral in the second row.

From the polynomial expansion for hematite (Table 1), it follows 10^3 ($\ln {}^{56/54}\beta_{\text{Hem}}(22°\text{C}) - \ln {}^{56/54}\beta_{\text{Hem}}(98\ °\text{C})) = 2.8$. According to Eq. (9), one can get $\Delta^{56/54}\text{Fe}_{\text{Fe(III)aq-hem}}$ $(22\ °\text{C}) = +0.47$. This gives a hematite–magnetite iron isotope fractionation at 22 °C:

$$\begin{aligned}\Delta^{56/54}\text{Fe}_{\text{hem-mag}} &= -\Delta^{56/54}\text{Fe}_{\text{Fe(III)aq-hem}} \\ &\quad + \Delta^{56/54}\text{Fe}_{\text{Fe(III)aq–Fe(II)aq}} \\ &\quad + \Delta^{56/54}\text{Fe}_{\text{Fe(II)aq-mag}} \\ &= 1.23‰. \end{aligned} \tag{10}$$

INRXS- and Mössbauer-derived polynomials in Table 1 give:

$$\begin{aligned}\Delta^{56/54}\text{Fe}_{\text{hem-mag}} &= 10^3(\ln {}^{56/54}\beta_{\text{hem}} - \ln {}^{56/54}\beta_{\text{mag}}) \\ &= 0.90‰. \end{aligned} \tag{11}$$

Similarly, one can compare equilibrium iron isotope fractionation between siderite and magnetite from INXRS and Mössbauer data with that obtained from laboratory experiment. Wiesli et al. (2004) obtained $\Delta^{56/54}\text{Fe}_{\text{Fe(II)aq-sid}} = +0.5‰$ for the ${}^{56/54}$Fe fractionation factor between ferrous aqua complexes and siderite at 22 °C. Combining this value with $\Delta^{56/54}\text{Fe}_{\text{Fe(II)aq-mag}} = -1.3‰$ from Johnson et al. (2005), one can get:

$$\begin{aligned}\Delta^{56/54}\text{Fe}_{\text{sid-mag}} &= \Delta^{56/54}\text{Fe}_{\ \text{Fe(II)aq-mag}} \\ &\quad - \Delta^{56/54}\text{Fe}_{\text{Fe(II)aq-sid}} \\ &= -1.3‰ - 0.5‰ = -1.8‰. \end{aligned} \tag{12}$$

The β-factor for siderite computed by Polyakov and Mineev (2000) from the Mössbauer-derived SOD shift and the INRXS-derived β-factor for magnetite give for equilibrium ${}^{56/54}$Fe isotope fractionation coefficient:

$$\begin{aligned}\Delta^{56/54}\text{Fe}_{\text{sid-mag}} &= 10^3(\ln {}^{56/54}\beta_{\text{sid}} - \ln {}^{56/54}\beta_{\text{mag}}) \\ &= -2.60‰. \end{aligned} \tag{13}$$

One can see from comparisons of Eq. (10) with Eq. (11) and (12) with Eq. (13) that the β-factors presented in this study slightly underestimate low-temperature hematite–magnetite and siderite–magnetite iron isotope fractionation coefficients relative to laboratory derived values. A possible reason for this disagreement is the magnetite sample used in the INRXS synchrotron radiation experiment by Seto et al. (2003). This sample was somewhat oxidized and the ratio between the tetrahedral (Fe^{3+}) A site and the octahedral ($\text{Fe}^{2+} + \text{Fe}^{3+}$) B site was 1.3:1 instead of 1:1 as in stoichiometric magnetite. Considering the dependence of the iron β-factor on oxidation state, the INRXS-derived iron β-factors for magnetite presented in this study might have overestimated those for stoichiometric magnetite. Mössbauer investigations of two stoichiometric magnetite samples (Mineev et al., 2007) support this assumption. At room temperature Mössbauer-derived $10^3\ln {}^{56/54}\beta$ for stoichiometric magnetite is 0.52 ± 0.35 smaller than that calculated in present study from INRXS data by Seto et al. (2003). Unfortunately, the A/B ratio in magnetite was not measured directly in experiments by Johnson et al. (2005).

A second possible reason for the disagreement between laboratory experiments and INRXS-and Mössbauer derived iron isotope fractionation factors deals with experimental procedure. All experimental data used in our comparisons, except $\Delta^{56/54}\text{Fe}_{\text{Fe(III)aq–Fe(II)aq}}$, were obtained in experiments involving mineral precipitation. Such experiments cannot unambigously demonstrate the attainment of isotopic equilibrium (e.g., O'Neil, 1986). On this ground, we cannot exclude the kinetic contribution in the values of the iron isotope fractionation coefficients obtained in the low-temperature experiments by Skulan et al. (2002), Wiesli et al. (2004), and Johnson et al. (2005).

4.3. Fe-bearing sulfide minerals

New INRXS and Mössbauer data have extended the range of the iron β-factors for sulfide minerals significantly (Fig. 10). Among sulfides, pyrite has the largest iron β-factor according to Mössbauer spectroscopy data. Unfortunately, because an INRXS-derived PDOS is not available for pyrite, the Mössbauer-derived large β-factors cannot be verified independently. However, we can test the validity of Mössbauer-derived iron β-factors of sulfide minerals, using their sulfur isotopes. Polyakov and Mineev (2000) calculated the sulfur β-factor of pyrite by Eq. (14) in which the kinetic energy of the sulfur sublattice in pyrite was written as the difference between the total kinetic energy of the crystal and the kinetic energy of the iron sublattice:

$$\ln \beta_{34/32S} = \frac{1}{17}\left(\frac{\text{KE}_{\text{tot}} - \text{KE}_{\text{Fe}}}{2RT} - \frac{3}{2}\right) \tag{14}$$

where KE_{tot} and KE_{Fe} are the kinetic energy of the total pyrite crystal and its iron sublattice, respectively, and 1/17 is a $\Delta m/m^*$ value for the ${}^{32}\text{S} \rightarrow {}^{34}\text{S}$ substitution that is under consideration. The total energy of the pyrite crystalline lattice was calculated from experimental data on the heat capacity of pyrite reported by Ogawa (1976). The iron sublattice kinetic energy was computed from the Mössbauer SOD shift data of Nishihara and Ogawa (1979). Polyakov and Mineev (2000) found good agreement in the sulfur isotope β-factors for pyrite between calculations according to Eq. (14) and those obtained by conventional statistical mechanical calculations. Here we further tested the validity of the sulfur β-factor values for pyrite, by comparing with experimentally calibrated sulfur isotope geothermometers: pyrite (FeS_2)–sphalerite (ZnS)–galena (PbS). The fractionation factors between pyrite–galena and pyrite–sphalerite can be obtained from sulfur β-factors for pyrite, galena and sphalerite, according to Eq. (1). The latter β-factors (galena and sphalerite) were calculated by Elcombe and Hulston (1975) using the lattice dynamic technique (Fig. 13a). Comparisons of calculated equilibrium fractionation factors for pyrite–galena and pyrite–sphalerite with appropriate experimental calibrations are presented in Fig. 13b. A good agreement between calculated and experimental values is observed. One can also estimate how much possible errors in values of the iron β-factor affect the sulfur β-factor for pyrite and calculated equilibrium fractionation factors for pyrite–galena and pyrite–sphalerite (Fig. 13b). Equation for ${}^{56/54}$Fe β-factor is written as

$$\ln \beta_{^{56/54}\mathrm{Fe}} = \frac{1}{27}\left(\frac{\mathrm{KE}_{\mathrm{Fe}}}{RT} - \frac{3}{2}\right). \qquad (15)$$

Combining Eqs. (14) and (15), one can derive dependence of the variation in $^{34/32}$S β-factor on the variation in the $^{56/54}$Fe β-factor after routine algebraic transformations:

$$\Delta(\ln \beta_{^{34/32}\mathrm{S}}) = \frac{27}{34}\Delta(\ln \beta_{^{56/54}\mathrm{Fe}}), \qquad (16)$$

where $\Delta(\ln \beta_{^{34/32}\mathrm{S}})$ and $\Delta(\ln \beta_{^{56/54}\mathrm{Fe}})$ are variations in $\ln \beta_{^{34/32}\mathrm{S}}$ and $\ln \beta_{^{56/54}\mathrm{Fe}}$, respectively. As it follows from Eq. (16) and Fig. 13b, even 2–3‰ variations in the $^{56/54}$Fe for pyrite lead to significant deviations of calculated pyrite–galena and pyrite–sphalerite equilibrium fractionation curves from appropriate experimental values.

The agreement between calculated equilibrium fractionation factors for pyrite–galena and pyrite–sphalerite and appropriate experimental calibrations (Fig. 13b) suggests strongly that the sulfur β-factor values for pyrite calculated by Eq. (14), and thus the iron β-factors of pyrite computed by Polyakov and Mineev (2000) using the Mössbauer SOD shift are accurate. In a similar fashion, we calculated the oxygen isotope β-factors of cassiterite (SnO_2) and found excellent agreement with fractionation factors determined by laboratory experiments (Hu et al., 2005; Polyakov et al., 2005a). Recently, Macey and Harris (2006) tested these oxygen isotope β-factors for cassiterite using natural samples and observed consistency of results obtained with quartz–cassiterite and quartz–hematite and quartz–muscovite isotope geothermometers.

Troilite shows the smallest value of the iron β-factor among sulfides studied to date. The iron β-factor of Fe_3S is very close to that of troilite. The small values of the iron β-factor for troilite are in agreement with results from the direct iron isotope exchange experiments in the pyrrhotite–peralkaline rhyolitic melt system at high temperature (Schuessler et al., 2005, 2007), assuming similarity between iron β-factors of troilite and pyrrhotite. According to these experiments an equilibrium fractionation factor between pyrrhotite and high Fe^{3+} peralkaline rhyolitic melt varies from −0.15 to −0.22‰/amu at temperatures from 850 to 1000 °C (Schuessler et al., 2005, 2007). These values of the iron isotope fractionation factor are close to those obtained from the typical values for the Mössbauer- and INRXS-derived iron β-factors of ferric silicates and troilite. Butler et al. (2005) suggested in their experimental study of Fe isotope fractionation on the precipitation of FeS that the enrichment of light iron isotopes in pyritic sediments can be explained by a kinetic isotope effect in the precipitation of FeS, followed by the conversion of FeS to pyrite without isotope fractionation. If we can assume that the β-factor of the monosulfide (mackinawite?) is similar to that of troilite, one can conclude that the enrichment of pyrite in light iron isotopes may be the result of equilibrium iron isotope fractionation during the precipitation of FeS on the first stage of the mechanism suggested by Butler et al. (2005). The small values of iron β-factors of troilite and Fe_3S obtained from INRXS extend the range of variations of the equilibrium iron isotope fractionation factors for covalently bonded compounds and open new possibilities for interpreting iron isotope ratios observed in nature.

5. SUMMARY

The critical reevaluation of equilibrium iron isotope fractionation factors has been accomplished for oxide and sulfide minerals, using recent literature data from Mössbauer spectroscopy and INRXS synchrotron radiation. Good agreement between iron β-factor values obtained

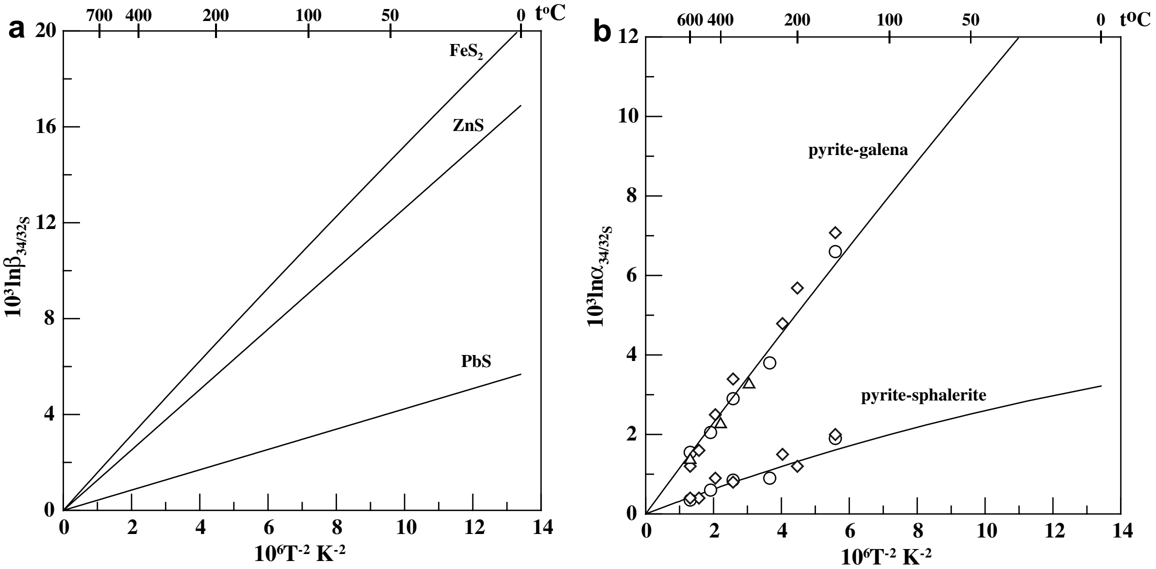

Fig. 13. Sulfur-isotope data of Fe-bearing sulfide minerals. (a) Temperature dependence of the $^{34/32}$S b-factor for pyrite taken from Polyakov and Mineev (2000) using the Mössbauer SOD shift for iron measured by Nishihara and Ogawa (1979). $^{34/32}$S β-factors for galena and sphalerite are taken from lattice dynamics calculations by Elcombe and Hulston (1975). (b) $^{34/32}$S equilibrium fractionation coefficients for pyrite–galena and pyrite–sphalerite pairs (solid lines) calculated from the appropriate β-factors in this figure (a) are presented in comparison with data by Smith et al. (1977) (open circles), Kajiwara et al. (1969) (open diamonds) and Kajiwara and Krouse (1971) (open triangles).

from the Mössbauer SOD shift and those obtained from the INRXS synchrotron radiation technique provides evidence for the validity and reliability of the iron β-factors for metallic iron (α-Fe) and hematite. Based on the excellent agreement between Mössbauer- and INRXS-derived iron β-factors for hematite, we suggest the use of hematite as a reference material.

New iron β-factors for magnetite have been computed from DOS obtained from the INRXS synchrotron radiation experiment (Seto et al., 2003). It is shown that the previous data on iron β-factors of magnetite computed by Polyakov and Mineev (2000) using the Mössbauer SOD shift of De Grave et al. (1993) and Persoons et al. (1993) are incorrect. The new data of magnetite resolve the disagreement between naturally observed iron isotope fractionation factors for mineral pairs involving magnetite and those calculated using the data from Mössbauer spectroscopy and INRXS. The validity of the iron β-factor for pyrite was corroborated, using sulfur isotope geothermometers of pyrite–galena and pyrite–sphalerite.

A correlation between the potential energy of the cation site and the iron β-factor value has been established. This correlation explains the dependence of the iron β-factors on the oxidation state: the iron potential energy of ferric compounds is about twice that of ferrous compounds. This correlation between the β-factor and the oxidation state could be extended to other transition metals (Cu, Sn, Mo, etc.).

Low values of INRXS-derived iron β-factors for troilite and Fe_3S have significantly widened the range of the iron β-factor values for sulfides, and for covalently bonded compounds in general. Observed low values of the iron β-factor of covalently bonded compounds agree with experimental study of pyrrhotite–silicate melt isotope exchange (Schuessler et al., 2005, 2007).

ACKNOWLEDGMENTS

Valuable comments by AE T. Chacko and constructive reviews by C.M.Johnson and E.A.Shauble promoted significant improvements of the paper, especially, the discussion chapter. We are particularly grateful to Dr. J.F. Lin for numerical data on Fe_3S PDOS. V.B.Polyakov and S.D.Mineev acknowledge support of Scientific Program # 7 of the Geoscience Department of Russian Academy of Sciences. Research was supported in part by an appointment to the Higher Education Research Experience at the Oak Ridge National Laboratory for Faculty, sponsored by U.S. DOE and administered by the Oak Ridge Institute for Science and Education. J. Horita was sponsored by the Division of Chemical Sciences, Geosciences, and Biosciences, Office of Basic Energy Sciences, U.S. Department of Energy, under contract DE-AC05-00OR22725, Oak Ridge National Laboratory, managed by UT-Battelle, LLC. R.N.Clayton acknowledges support of the NSF through grant EAR-0439925.

REFERENCES

Alp E. E., Sturhahn W. and Toellner T. S. (2001) Lattice dynamics and inelastic nuclear resonant X-ray scattering. *J. Phys.: Condens. Matter* **13**, 7645–7658.

Anbar A. D. (2004) Iron stable isotopes: beyond biosignatures. *Earth Planet. Sci. Lett.* **217**, 223–236.

Anbar A. D., Jarzeski A. A. and Spiro T. G. (2005) Theoretical investigation of iron isotope fractionation between $Fe(H_2O)_6{}^{3+}$ and $Fe(H_2O)_6{}^{2+}$: implications for iron stable isotope geochemistry. *Geochim. Cosmochim. Acta* **69**, 825–837.

Balci N., Bullen T. D., Witte-Lien K., Shanks W. C., Motelica M. and Mandernack K. W. (2006) Iron isotope fractionation during microbially stimulated Fe(II) oxidation and Fe(III) precipitation. *Geochim. Cosmochim. Acta* **70**, 622–639.

Beard B. L. and Johnson C. M. (2004a) Fe isotope variations in the modern and ancient Earth and other planetary bodies. *Rev. Mineral. Geochem.* **55**, 319–357.

Beard B. L. and Johnson C. M. (2004b) Inter-mineral Fe isotope variations in mantle-derived rocks and implications for the Fe geochemical cycle. *Geochim. Cosmochim. Acta* **68**, 4727–4743.

Bertka C. M. and Fei Y. (1998) Implications of Mars Pathfinder data for the accretion history of the terrestrial planets. *Science* **281**, 1838–1840.

Bigeleisen J. and Mayer M. G. (1947) Calculation of equilibrium constants for isotope exchange reactions. *J. Chem. Phys.* **15**, 261–267.

Brantley S. L., Liermann L. and Bullen T. D. (2001) Fractionation of Fe isotopes by soil microbes and organic acids. *Geology* **29**, 535–538.

Busigny V. and Dauphas N. (2007) Tracing paleofluid circulations using iron isotopes: a study of hematite and goethite concretions from the Navajo Sandstone (Utah, USA). *Earth Planet. Sci. Lett.* **254**, 272–287.

Butler I. B., Archer C., Vance D., Oldroyd A. and Rickard D. (2005) Fe isotope fractionation on FeS formation in ambient aqueous solution. *Earth Planet. Sci. Lett.* **236**, 230–242.

Chacko T., Hu X. S., Mayeda T. K., Clayton R. N. and Goldsmith J. R. (1996) Oxygen isotope fractionation in muscovite, phlogopite and rutile. *Geochim. Cosmochim. Acta* **60**, 2595–2608.

Chumakov A. I., Rüffer R., Baron A. Q. R., Grünsteudel H. and Grünsteudel H. F. (1996) Temperature dependence of nuclear inelastic absorption of synchrotron radiation in alpha-Fe-57. *Phys. Rev.* **B54**, R9596.

Chumakov A. I. and Sturhahn W. (1999) Experimental aspects of inelastic nuclear resonance scattering. *Hyp. Interact.*(123/124), 781–808.

Clayton R. N., Goldsmith J. R. and Mayeda T. K. (1989) Oxygen isotope fractionation in quartz, albite, anorthite, and calcite. *Geochim. Cosmochim. Acta* **53**, 725–733.

Croal L. R., Johnson C. M., Beard B. L. and Newman D. K. (2004) Iron isotope fractionation by Fe(II)-oxidizing photoautotrophic bacteria. *Geochim. Cosmochim. Acta* **68**, 1227–1242.

Dauphas N. and Rouxel O. (2006) Mass spectrometry and natural variations of iron isotopes. *Mass Spectrom. Rev.* **25**, 515–550.

Dauphas N., van Zuilen M., Wadhwa M., Davis A. M., Marty B. and Janney P. E. (2004) Clues from Fe isotope variations on the origin of early Archean BIFs from Greenland. *Science* **306**, 2077–2080.

Dauphas N., Cates N. L., Mojzsis S. J. and Busigny V. (2007) dentification of chemical sedimentary protoliths using iron isotopes in the >3750 Ma Nuvvuagittuq supracrustal belt, Canada. *Earth Planet. Sci. Lett.* **254**, 358–376.

De Grave E. and Van Alboom A. (1991) Evaluation of ferrous and ferric Mössbauer fractions. *Phys. Chem. Minerals* **18**, 337–342.

De Grave E., Persoons R. M., Vandenberghe R. E. and De Bakker P. M. A. (1993) Mössbauer study of the high-temperature phase of Co-substituted magnetites, $Co_xFe_{3-x}O_4$. I. $x \leqslant 0.04$. *Phys. Rev.* **B47**, 5881–5893.

Dideriksen K., Baker J. A. and Stipp S. L. S. (2006) Iron isotopes in natural carbonate minerals determined by MC-ICP-MS with a Fe-58-Fe-54 double spike. *Geochim. Cosmochim. Acta* **70**, 118–132.

Elcombe M. M. and Hulston J. R. (1975) Calculation of sulphur isotope fractionation between sphalerite and galena using lattice dynamics. *Earth Planet. Sci. Lett.* **28**, 172–180.

Frost C. D., von Blanckenburg F., Schoenberg R., Frost B. R. and Swapp S. M. (2007) Preservation of Fe isotope heterogeneities during diagenesis and metamorphism of banded iron formation Contrib. *Min. Petrol.* **153**, 211–235.

Horn I., von Blanckenburg F., Schoenberg R., Steinhoefel G. and Markl G. (2006) In situ iron isotope ratio determination using UV-femtosecond laser ablation with application to hydrothermal ore formation processes. *Geochim. Cosmochim. Acta* **70**, 3677–3688.

Housley R. M. and Hess F. (1967) Analyses of Debye–Waller-factor and Mössbauer-thermal-shift measurements II. Thermal-shift data on Fe. *Phys. Rev.* **164**, 340–344.

Hu G., Clayton R. N., Polyakov V. B. and Mineev S. D. (2005) Oxygen isotope fractionation factors involving cassiterite (SnO_2): II. Determination by direct exchange between cassiterite and calcite. *Geochim. Cosmochim. Acta* **69**, 1301–1305.

Jarzęcki A. A., Anbar A. D. and Spiro T. G. (2004) DFT analysis of $Fe(H_2O)_6{}^{3+}$ and $Fe(H_2O)_6{}^{2+}$ structure and vibrations; implications for isotope fractionation. *J. Phys. Chem. A* **108**, 2726–2732.

Johnson C. M., Beard B. L., Beukes N. J., Klein C. and O'Leary J. M. (2003) Ancient geochemical cycling in the Earth as inferred from Fe isotope studies of banded iron formations from the Transvaal Craton. *Contrib. Mineral. Petrol.* **144**, 523–547.

Johnson C. M., Beard B. L., Roden E. E., Newman D. K. and Nealson K. H. (2004a) Isotopic constraints on biochemical cycling of Fe. *Rev. Mineral. Geochem.* **55**, 359–408.

Johnson C. M., Beard B. L., and Albarède F. (Eds.) (2004) Geochemistry of non-traditional stable isotopes. *Rev. Min. Geochem.* **55**.

Johnson C. M., Roden E. E., Welch S. A. and Beard B. L. (2005) Experimental constraints on Fe isotope fractionation during magnetite and Fe carbonate formation coupled to dissimilatory hydrous ferric oxide reduction. *Geochim. Cosmochim. Acta* **69**, 963–993.

Kajiwara Y. and Krouse H. R. (1971) Sulfur isotope partitioning in metallic sulfide system. *Can. J. Earth Sci.* **8**, 1397–1408.

Kajiwara Y., Krouse H. R. and Sasaki A. (1969) Experimental study of sulfur isotope fractionation between coexistent sulfide minerals. *Earth Planet. Sci. Lett.* **7**, 271–277.

Kobayashi H., Kamimura T., Alfè D., Sturhahn W., Zhao J. and Alp E. E. (2004) Phonon density of states and compression behavior in iron sulfide under pressure. *Phys. Rev. Lett.* **93**, 195503-1–195503-4.

Kohn V. G. and Chumakov A. I. (2000) DOS: Evaluation of phonon density of states from nuclear resonant inelastic absorption. *Hyp. Interact.* **125**, 205–221.

Kohn V. G., Chumakov A. I. and Rüffer R. (1998) Nuclear resonant inelastic absorption of synchrotron radiation in an anisotropic single crystal. *Phys. Rev. B* **58**, 8437–8444.

Lin J. F., Fei Y., Sturhahn W., Zhao J., Mao H. and Hemley R. J. (2004) Magnetic transition and sound velocities of Fe_3S at high pressure: implications for Earth and planetary cores. *Earth Planet. Sci. Lett.* **226**, 33–40.

Macey P. and Harris C. (2006) Stable isotope and fluid inclusion evidence for the originof the Brandberg West area Sn–W vein deposits, NW Namibia. *Miner. Deposita* **41**, 671–690.

Maradudin A. A., Montroll E. W., Weiss G. H. and Ipatova I. P. (1971) *Theory of Lattice Dynamics in the Harmonic Approximation. Solid State Physics*. Academic Press, New York.

Markl G., Von Blanckenburg F. and Wagner T. (2006) Iron isotope fractionation during hydrothermal ore deposition and alteration. *Geochim. Cosmochim. Acta* **70**, 3011–3030.

Matthews A., Zhu X.-K. and O'Nions R. K. (2001) Kinetic iron stable isotope fractionation between iron (-II) and (-III) complexes in solution. *Earth Planet. Sci. Lett.* **192**, 81–92.

Matthews A., Morgans-Bell H. S., Emmanuel S., Jenkyns H. C., Erel Y. and Halicz L. (2004) Controls on iron-isotope fractionation in organic-rich sediments (Kimmeridge Clay, Upper Jurassic, southern England). *Geochim. Cosmochim. Acta* **68**, 3107–3123.

Mineev S. D., Polyakov V. B., and Permyakov Y. V. (2007) Equilibrium iron isotope fractionation factors for magnetite from Mössbauer spectroscopy and inelastic nuclear resonant X-ray scattering data. *Geochim. Cosmochim. Acta* **71**, Supplement (in press).

Nishihara Y. and Ogawa S. (1979) Mössbauer study ^{57}Fe in pyrite-type dichalcogenides. *J. Chem. Phys.* **71**, 3796–3801.

Ogawa S. (1976) Specific heat study of magnetic ordering and band structure of 3d transition metal disulfides having pyrite structure. *J. Phys. Soc. Jpn.* **41**, 462–469.

O'Neil J. R. (1986) Theoretical and experimental aspects of isotopic fractionation. In *Stable Isotopes in High Temperature Geological Processes*, Rev. Mineral. vol. 16 (eds. J. W. Valley, H. P. Taylor, Jr., and J. R. O'Neil), pp. 1–40.

Permyakov Yu. V., Polyakov V. B., and Mineev S. D. (2004) Determination of the iron β-factor for pyrite from the Moessbauer spectroscopy data. In *XVII A.P. Vinogradov Symposium on Isotope Geochemistry. 6–9 December Moscow, Abstracts*. pp. 189–190 (in Russian).

Persoons R. M., De Grave E., de Bakker P. M. A. and Vandenberghe R. E. (1993) Mössbauer study of the high-temperature phase of Co-substituted magnetites, $Co_xFe_{3-x}O_4$. II. $x \geqslant 0.1$. *Phys. Rev.* **B47**, 5894–5905.

Poirier J. P. (1994) Light elements in the Earth's core: a critical review. *Phys. Earth Planet. Inter.* **85**, 319–337.

Poitrasson F., Halliday A. N., Lee D.-C., Levasseur S. and Teutsch N. (2004) Iron isotope differences between Earth, Moon, Mars and Vesta as possible records of contrasted accretion mechanisms. *Earth Planet. Sci. Lett.* **223**, 253–266.

Poitrasson F., Levasseur S. and Teutsch N. (2005) Significance of iron isotope mineral fractionation in pallasites and iron meteorites for the core–mantle differentiation of terrestrial planets. *Earth Planet. Sci. Lett.* **234**, 151–164.

Polyakov V. B. (1993) On ideality of isotope mixture in solids. *Russ. J. Phys. Chem.* **67**, 422–425.

Polyakov V. B. (1997) Equilibrium fractionation of the iron isotopes: estimation from Mössbauer spectroscopy data. *Geochim. Cosmochim. Acta* **61**, 4213–4217.

Polyakov V. B. and Kharlashina N. N. (1994) Effect of pressure on equilibrium isotopic fractionation. *Geochim. Cosmochim. Acta* **58**, 4739–4750.

Polyakov V. B. and Kharlashina N. N. (1995) The use of heat capacity data to calculate carbon isotope fractionation between graphite, diamond, and carbon dioxide: A new approach. *Geochim. Cosmochim. Acta* **59**, 2561–2572.

Polyakov V. B. and Mineev S. D. (2000) The use of Mössbauer spectroscopy in stable isotope geochemistry. *Geohim. Cosmochim. Acta* **64**, 849–865.

Polyakov V. B., Mineev S. D., Clayton R. N. and Hu G. (2005a) Oxygen isotope equilibrium factors involving cassiterite (SnO_2): I. Calculation of reduced partition function ratios from heat capacity and X-ray resonant studies. *Geochim. Cosmochim. Acta* **69**, 1287–1300.

Polyakov V. B., Mineev S. D., Clayton R. N., Hu G. and Mineev K. S. (2005b) Determination of tin equilibrium isotope fractionation factors from synchrotron radiation experiments. *Geochim. Cosmochim. Acta* **69**, 5531–5536.

Polyakov V. B., Mineev S. D., Gurevich V. M., Khramov D. A., Gavrichev K. S., Gorbunov V. E. and Golushina L. N. (2001)

The use of Mössbauer spectroscopy and calorimetry for determining isotopic equilibrium constants. Hematite. *Russ. J. Phys. Chem.* **75**, 912–916.

Rosenbaum J. M., Mattey D. P. and Elphick S. (1994) Equilibrium garnet–calcite oxygen isotopic fractionation. *Mineral. Mag.* **58A**, 787–788.

Roskosz M., Luais B., Watson H. C., Toplis M. J., Alexander C. M. O'D. and Mysen B. O. (2006) Experimental quantification of the fractionation of Fe isotopes during metal segregation from a silicate melt. *Earth Planet. Sci. Lett.* **248**, 851–867.

Rouxel O., Dobbek N., Fouquet Y. and Ludden J. N. (2003) Iron isotope fractionation during oceanic crust alteration. *Chem. Geol.* **202**, 155–182.

Rouxel O., Fouquet Y. and Ludden J. N. (2004) Subsurface processes at the Lucky Strike hydrothermal field, Mid-Atlantic Ridge: evidence from sulfur, selenium, and iron isotopes. *Geochim. Cosmochim. Acta* **68**, 2295–2311.

Rouxel O. J., Bekker A. and Edwards K. J. (2005) Iron isotope constraints on the archean and paleoproterozoic ocean redox state. *Science* **307**, 1088–1091.

Schauble E. A., Rossman G. R. and Taylor H. P. (2001) Theoretical estimates of equilibrium Fe isotope fractionations from vibrational spectroscopy. *Geochim. Cosmochim. Acta* **65**, 2487–2597.

Schoenberg R. and Von Blanckenburg F. (2004) An assessment of the accuracy of stable Fe isotope ratio measurements on samples with organic and inorganic matrices by high-resolution multicollector ICP-MS. *Int. J. Mass Spectrom.* **242**, 257–272.

Schoenberg R. and von Blanckenburg F. (2006) Modes of planetary-scale Fe isotope fractionation. *Earth and Planet. Sci. Lett.* **252**, 342–359.

Schuessler J., Schoenberg R., Behrens H. and Von Blanckenburg F. (2005) Experimental calibration of the Fe isotope fractionation between pyrrhotite and silicate melt. *Geochim. Cosmochim. Acta* **69**(Suppl. 1), A211.

Schuessler J. A., Schoenberg R., Behrens H. and von Blanckenburg F. (2007) The experimental calibration of the iron isotope fractionation factor between pyrrhotite and peralkaline rhyolitic melt. *Geochim. Cosmochim. Acta* **71**, 417–433.

Seto M., Kitao S., Kobayashi Y., Haruki R., Yoda Y., Mitsui T. and Ishikawa T. (2003) Site-specific phonon density of states discerned using electronic states. *Phys. Rev. Lett.* **91**, 185505-1–185505-4.

Severmann S., Johnson C. M., Beard B. L. and McManus J. (2006) The effect of early diagenesis on the Fe isotope compositions of porewaters and authigenic minerals in continental margin sediments. *Geochim. Cosmochim. Acta* **70**, 2006–2022.

Shen G., Sturhahn W., Alp E. E., Zhao J., Toellner T. S., Prakapenka V. B., Meng Y. and Mao H.-K. (2004) Phonon density of states in iron at high pressures and high temperatures. *Phys. Chem. Minerals* **31**, 353–359.

Singh R. K. and Wolfsberg M. (1975) The calculation of isotopic partition functions ratio by perturbation theory technique. *J. Chem. Phys.* **62**, 4165–4180.

Skulan J. L., Beard B. L. and Johnson C. M. (2002) Kinetic and equilibrium Fe isotope fractionation between aqueous Fe(III) and hematite. *Geochim. Cosmochim. Acta* **66**, 2995–3015.

Smith J. W., Doolan S. and McFarlane E. F. (1977) A sulfur isotope geothermometerfor the trisulfide system galena–sphalerite–pyrite. *Chem. Geol.* **19**, 83–90.

Smyth J. R. (1989) Electrostatic characterization of oxygen sites in minerals. *Geochim. Cosmochim. Acta* **53**, 1101–1110.

Smyth J. R. and Bish D. L. (1988) *Crystal Structures and Cation Sites in the Rock-forming Minerals*. Routledge.

Smyth J. R. and Clayton R. N. (1988) Correlation of oxygen isotope fractionations and electrostatic site potentials in silicates. *Eos* **69**, 1514.

Struzhkin V. V., Mao H.-K., Mao W. L., Hemley R. J., Sturhahn W., Alp E. E., L'Abbe C., Hu M. Y. and Errandonea D. (2004) Phonon density of states and elastic properties of Fe-based materials under compression. *Hyp. Interac.* **153**, 3–15.

Struzhkin V. V., Mao H. K., Hu J. Z., Schwoerer-Bohning M., Shu J. F., Hemley R. J., Sturhahn W., Hu M. Y., Alp E. E., Eng P. and Shen G. Y. (2001) Nuclear inelastic X-ray scattering of FeO to 48 GPa. *Phys. Rev. Lett.* **87**, 255501-1–255501-4.

Sturhahn W., Alp E. E., Toellner T. S., Hession P., Hu M. and Sutter J. (1998) Introduction to nuclear resonant scattering with synchrotron radiation. *Hyp. Interact.* **113**, 47–58.

Sturhahn W., Toellner T. S., Alp E. E., Zhang X. W., Yoda Y., Kikuta S., Seto M., Kimball C. W. and Dabrowski B. (1995) Phonon density of states measured by inelastic nuclear resonant scattering. *Phys. Rev. Lett.* **74**, 3832.

Toellner T. S., Hu M., Sturhahn W., Quast K. W. and Alp E. E. (1997) Inelastic nuclear resonant scattering with sub-meV energy resolution. *Appl. Phys. Lett.* **71**, 2112–2114.

Urey H. C. (1947) The thermodynamic properties of isotopic substances. *J. Chem. Soc. (London)*, 562–581.

Walczyk T. and Von Blanckenburg F. (2002) Natural iron isotope variations in human blood. *Science* **295**, 2065–2066.

Welch S. A., Beard B. L., Johnson C. M. and Braterman P. S. (2003) Kinetic and equilibrium Fe isotope fractionation between aqueous Fe(II) and Fe(III). *Geochim. Cosmochim. Acta* **67**, 4231–4250.

Wiesli R. A., Beard B. L. and Johnson C. M. (2004) Experimental determination of Fe isotope fractionation between aqueous Fe(II), siderite and "green rust" in abiotic systems. *Chem. Geol.* **211**, 343–362.

Williams H. M., McCammon C. A., Peslier A. H., Halliday A. N., Teutsch N., Levasseur S. and Burg J.-P. (2004) Iron isotope fractionation and the oxygen fugacity of the mantle. *Science* **304**, 1656–1659.

Williams H. M., Peslier A. H., McCammon C. A., Halliday A. N., Teutsch N., Levasseur S. and Burg J.-P. (2005) Systematic iron isotope variations in mantle rocks and minerals: The effects of partial melting and oxygen fugacity. *Earth Planet. Sci. Lett.* **235**, 435–452.

Yamaguchi K. E., Johnson C. M., Beard B. L. and Ohmoto H. (2005) Biogeochemical cycling of iron in the Archean-Paleoproterozoic Earth: Constraints from iron isotope variations in sedimentary rocks from the Kaapvaal and Pilbara Cratons. *Chem. Geol.* **218**, 135–169.

Associate editor: Thomas Chacko